

# Dual Linearly Polarized Microstrip Antenna Using a Slot-Loaded $TM_{50}$ Mode

Yijing He , Yue Li , Senior Member, IEEE, Wangyu Sun , Zhijun Zhang , Fellow, IEEE, and Pai-Yen Chen , Senior Member, IEEE

**Abstract**—We present a high-gain, low-profile dual-polarized microstrip antenna operating in the hybridized higher order mode. The proposed antenna consists of a slot-loaded cross-shaped patch, which can be considered as orthogonally polarized radiating elements operated in the  $TM_{50}$  mode. Moreover, the four loaded slots can effectively excite the in-phase  $TM_{10}$  mode such that the superposition of both modes can lead to gain enhancement in the broadside direction, with suppressed sidelobes. The proposed antenna requires only a single-dielectric layer and a simple feeding method, while exhibiting good isolation between the two polarizations. We have developed a prototype, which has a total size of only  $1.65 \lambda_0 \times 1.65 \lambda_0 \times 0.04 \lambda_0$  ( $\lambda_0$  is the free-space wavelength at the center frequency) and a measured maximum gain of 10.9 dBi. This dual-polarized microstrip antenna with the advantages of high gain, low profile, low cost, and good isolation, is envisioned to benefit many multiple-input, multiple-output and the fifth generation (5G) communication systems.

**Index Terms**—Dual-polarized antenna, high-gain low-profile antennas, higher order mode excitation, microstrip antenna.

## I. INTRODUCTION

A DUAL-POLARIZED antenna has been a very attractive choice for multiple-input multiple-output (MIMO) and the fifth generation (5G) communication systems, which can provide reduced Rayleigh fading, and drastically increased spectral efficiency and channel capacity [1]–[4]. To date, different types of dual-polarized antenna have been explored in the literature, with structures ranging from cross dipoles [5]–[8], slots [9]–[11], and magneto-electric dipoles [12]–[14], to microstrip antennas [15]–[19]. Microstrip antennas are most common types in modern wireless systems, as they offer many advantages such as low profile, low cost, ease of fabrication, and full integration with planar circuits [15]. In practice, it is rather challenging to design a high-gain, dual-polarized microstrip antenna. So far, several techniques have been proposed to increase the gain of microstrip antenna. In [20]–[22], the array configuration is

proposed to increase the directivity of antenna. This approach, however, requires the complex feed network, which could increase the design and fabrication complexity and could affect radiation properties.

A low-permittivity substrate [23], [24] and stacked parasitic patches [25]–[28], with reduced loss and enlarged radiating aperture, can also enhance gain and bandwidth performance of a microstrip antenna. The disadvantages of these approaches are, however, that the total size is increased. Recently, high-gain microstrip antennas operating at higher order modes have been proposed [29]–[31]. In [30], stacked circular patches were used to achieve the high-gain, low-sidelobe microstrip antennas designed to operate at  $TM_{11}$  and  $TM_{13}$  modes. In [31], a gain-enhanced, beam-adjustable patch antenna operating under the  $TM_{03}$  mode was proposed. Nonetheless, these high-gain antennas operated at higher order modes only cover one polarization.

In this letter, we propose a high-gain, low-profile, and dual-polarized microstrip antenna. This dual-polarized antenna employs a single-dielectric layer and a simple feed technique, with four identical slots loaded on the cross-shaped radiating patch. The antenna can be seen to be formed by a pair of identical horizontal and vertical patches (radiating elements) operating in the  $TM_{50}$  mode. For each polarization element, the collective effect of electric fields on the two slots can be equivalent to the  $TM_{10}$  mode, which oscillates in phase with the  $TM_{50}$  mode excited at both edges of the patch. Compared to conventional microstrip antenna operating in the fundamental mode, the gain enhancement is significant, while several exciting features are offered, including dual-polarized radiation, low profile, simple design, and good isolation.

## II. ANTENNA DESIGN

### A. Antenna Configuration

Fig. 1 shows the geometry of the proposed antenna, consisting of a cross-shaped printed patch with four etched slots on a grounded dielectric substrate (F4B, with relative permittivity of  $2.55 \pm 0.05$ , loss tangent of 0.001, and thickness of 2.0 mm). The proposed dual-polarized antenna is fed by two coaxial probes. The inner conductor of the coaxial cable is soldered to the cross-shaped patch, and the outer conductor is soldered to the ground plane. The location of the coaxial probe is offset from the center by a distance  $s$  (5.5 mm) to achieve good impedance matching. Detailed design parameters are summarized in Table I, which were optimized using the finite element method

Manuscript received August 2, 2018; accepted October 1, 2018. Date of publication October 8, 2018; date of current version November 29, 2018. This work was supported by the National Natural Science Foundation of China under Grant 61771280. (Corresponding author: Yue Li.)

Y. He, Y. Li, W. Sun, and Z. Zhang are with the Department of Electronic Engineering, Tsinghua University, Beijing 100084, China (e-mail: heyj16@mails.tsinghua.edu.cn; lyee@tsinghua.edu.cn; sunwy16@mails.tsinghua.edu.cn; zjzh@tsinghua.edu.cn).

P.-Y. Chen is with the Department of Electrical and Computer Engineering, University of Illinois at Chicago, Chicago, IL 60607 USA (e-mail: pychen@uic.edu).

Digital Object Identifier 10.1109/LAWP.2018.2874472

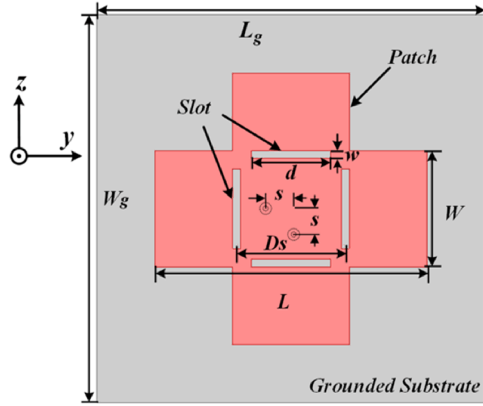


Fig. 1. Top view of the structure and the geometry of the proposed high-gain low-profile dual-polarized microstrip antenna.

TABLE I

DIMENSIONS OF THE PROPOSED DUAL-POLARIZED ANTENNA (UNIT: mm)

$L_g$	$W_g$	$L$	$W$	$s$	$D_s$	$d$	$w$	$H$
83	83	58.5	26.5	5.5	23.9	19	1.9	2

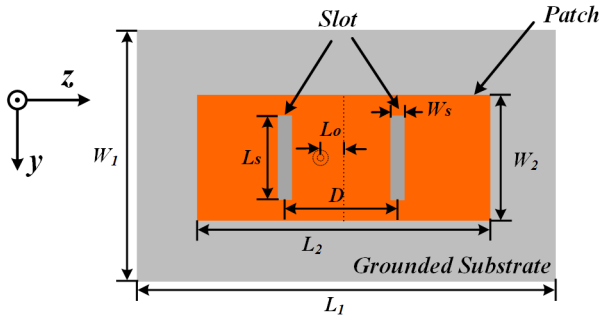


Fig. 2. Geometry of the proposed single-polarized microstrip antenna element working at  $TM_{50}$  mode ( $L_1 = 100$  mm,  $W_1 = 60$  mm,  $L_2 = 61$  mm,  $W_2 = 24$  mm,  $L_o = 4$  mm,  $D = 22.5$  mm,  $L_s = 17.8$  mm,  $W_s = 2.5$  mm,  $h = 2$  mm.).

solver, Ansoft high-frequency structure simulator. Fig. 2 shows the single-polarized design, whose geometry is similar to the dual-polarized one in Fig. 1, but using a slotted rectangular printed patch.

### B. Operating Principle

It is known that a microstrip antenna operating in higher order odd modes can exhibit a larger radiation aperture, compared with the fundamental ( $TM_{10}$ ) mode. When operated at the higher order odd mode, the distance between the two radiating edges of microstrip antenna is enlarged, and therefore, the peak gain in the broadside direction is enhanced. However, due to the enlarged spacing between the two radiating edges, the undesirable sidelobes are usually unavoidable. How to achieve simultaneously high gain and low sidelobe remains challenging for the microstrip antenna design.

As inspired by the design principle in [30], we first designed a high-gain, hybrid-mode single-polarized microstrip antenna, consisting of stacked rectangular patches, as shown in Fig. 3(a). A suspended patch operating in the  $TM_{10}$  mode is mounted

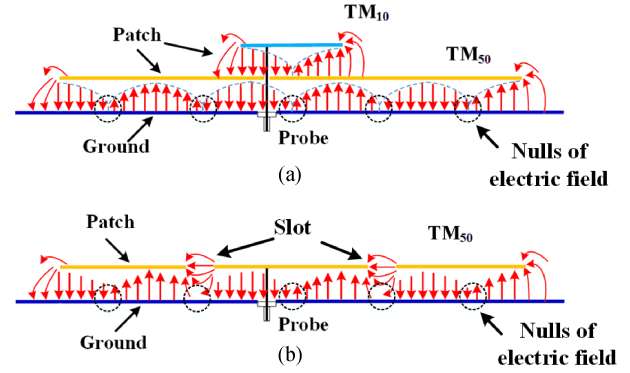


Fig. 3. Sketch of electric vector field distribution of (a) the dual-mode stacked microstrip antenna with upper patch working at  $TM_{10}$  mode and lower patch working at  $TM_{50}$  mode, and (b) the proposed single-polarized microstrip antenna element working at  $TM_{50}$  mode with two etched slots.

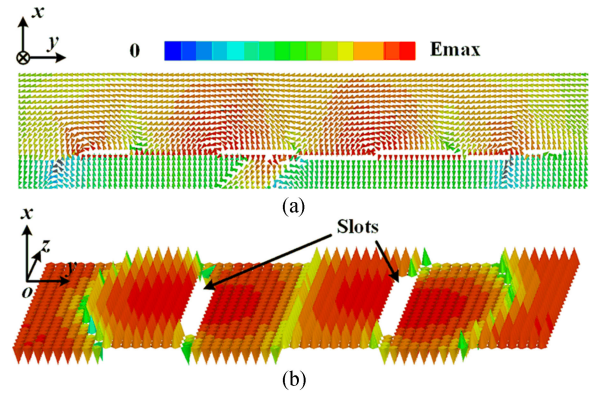


Fig. 4. Snapshot of electric vector field distribution in (a) E-plane of the proposed antenna at 5.96 GHz. (b) Perspective view.

on top of the second patch with a bigger size, operating in the  $TM_{50}$  mode. As can be understood from the schematic electric fields distribution in Fig. 3(a), currents induced on the top patch ( $TM_{10}$  mode) and bottom patch ( $TM_{50}$  mode) would oscillate in phase. The black dotted circles in Fig. 3 represent nulls of electric field, pointing out that the lower patch is operating at  $TM_{50}$  mode. The superposition of in-phase radiating edges of two patches can lead to the gain enhancement in the broadside direction, with very low sidelobes. However, this stacked configuration requires complex and costly fabrication.

In order to achieve the same performance with a low-profile, single-layered structure, we propose a new coplanar design in Fig. 2. Here, two slots are employed to replace the upper patch. Specifically, the two slots are etched at the transition points (i.e., nulls of electric field) of the lower patch, which can be directly observed from the simulated electric field distribution. The electrical distance between two slots is roughly a half of the operating wavelength. As illustrated in Fig. 3(b), the fringing electric fields on the two slots are polarized in-phase with the radiating edges of the patch. The superposition of radiation fields generated by magnetic currents induced on two slots ( $TM_{10}$  mode) and on patch's edges ( $TM_{50}$  mode) results in the enhancement of broadside gain and reduction of sidelobes. Fig. 4(a) shows the simulated snapshot of electric vector field distribution on the E-plane of the proposed microstrip antenna. The detailed geom-

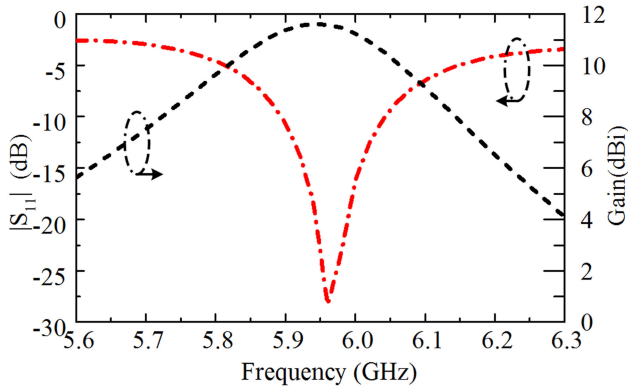


Fig. 5. Simulated  $S_{11}$  parameter and gain of the proposed single-polarized microstrip antenna element shown in Fig. 2.

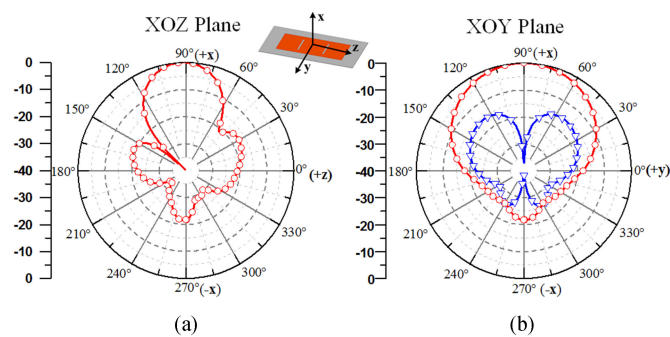


Fig. 6. Simulated normalized (a) E-plane and (b) H-plane pattern of the proposed single-polarized microstrip antenna element shown in Fig. 2.

erty and design parameters of this single-polarized antenna are reported in the caption of Fig. 2. Fig. 4(b) is similar to Fig. 4(a), but for the prospective view of the electric field distribution. The dual-polarized microstrip antenna shown in Fig. 1 can be decomposed into horizontal and vertical elements. It is clearly seen from Fig. 4 that a four-current mode, including two from loaded slots and two from edges of the patch, can be excited due to strong local fields polarized in opposite directions.

Fig. 5 reports the simulated  $S_{11}$  and gain for the proposed single-polarized antenna in Fig. 2. In the operating band (from 5.90 to 6.05 GHz), the antenna has a maximum gain of 11.5 dBi. Fig. 6(a) and (b) presents the simulated radiation patterns at 5.96 GHz for this antenna on the E-plane and the H-plane, respectively. The cross-polarization of the E-plane is too small to show in Fig. 6(a). It is seen from Fig. 6 that the antenna has a low sidelobe level of  $-17$  dB.

By combining two single-polarized radiating elements in Fig. 2, arranged in the form of cross configuration (see Fig. 1), a high-gain dual-polarized microstrip antenna can be developed. This dual-polarized antenna has a cross-shaped patch loaded with four slots (see Fig. 1). Fig. 7 illustrates the perspective view of the simulated snapshot of the electric field distribution at the center operating frequency; here, two ports are excited simultaneously. The null electric field observed in diagonal direction of the patch is due to the superposition of two polarizations. Although two orthogonal radiating elements overlap in the center region, the operating modes are nearly independent for two polarizations.

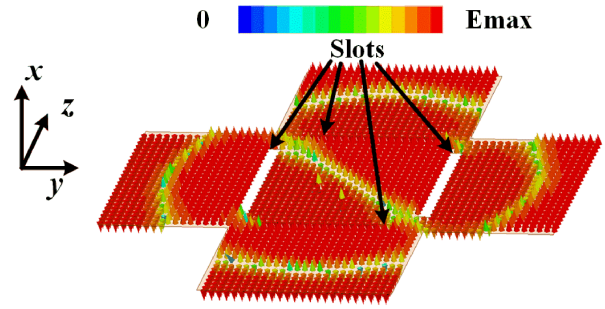


Fig. 7. Perspective view of the snapshot of an electric vector field distribution of the proposed dual-polarized antenna at 5.96 GHz.

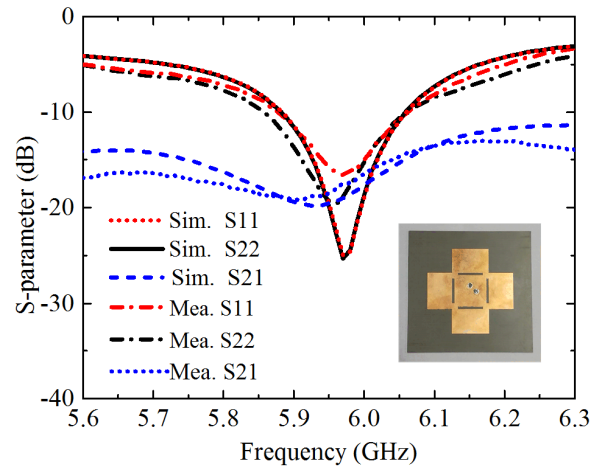


Fig. 8. Simulated measured  $S$ -parameters of the proposed dual-polarized microstrip antenna and the fabricated prototype.

### III. EXPERIMENTAL RESULTS

To verify the high-gain and low-profile signatures of the proposed dual-polarized antenna, a prototype was fabricated and shown in the inset of Fig. 8. The antenna was made by the standard printed circuits board technique. The dual-polarized antenna is fed by two  $50 \Omega$  coaxial cables. The  $S$ -parameters were measured by a vector network analyzer (Agilent E5071B), and the radiation patterns were measured in the far-field anechoic chamber.

#### A. $S$ -Parameters

Fig. 8 shows the simulated and measured  $S$ -parameters of the dual-polarized microstrip antenna. The measured  $-10$  dB impedance bandwidth covers from 5.88 to 6.06 GHz for both polarizations. The measured reflection coefficients of the two ports are almost identical and agree well with the simulation results. The difference between simulation and experimental results could be resulted from impedance mismatch between antenna and coaxial cables, fabrication errors, and fluctuations of material properties. We note that a good isolation between two feeding ports (less than  $-14$  dB) is obtained within the frequency band of interest. In fact, a higher isolation may be obtained by using the differential feeding method, which, however, requires a more complicated feeding network and a double-layered structure.

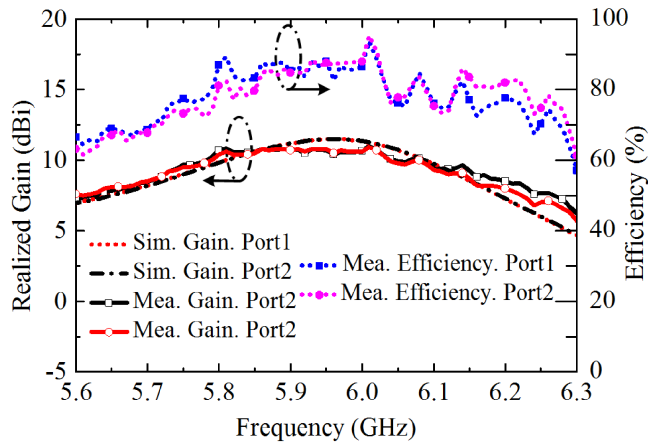


Fig. 9. Measured and simulated gain and efficiency of the two feeding ports of the proposed dual-polarized microstrip antenna.

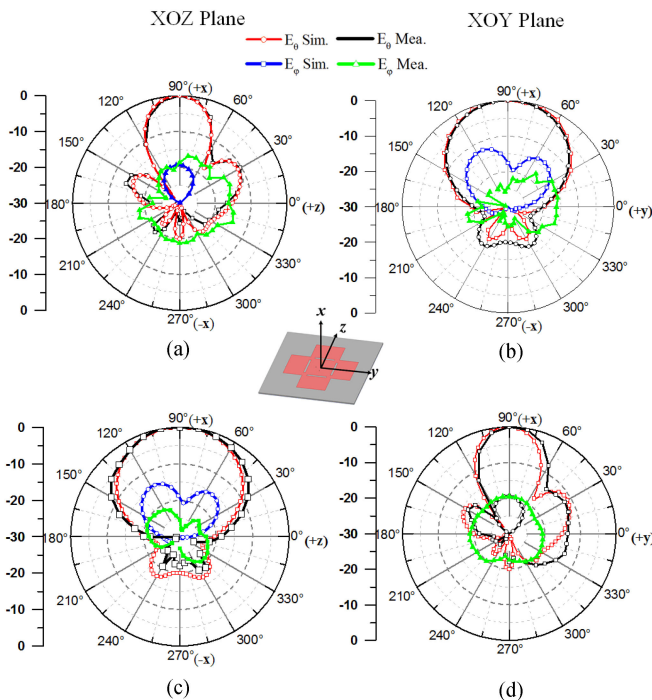


Fig. 10. Simulated and measured normalized radiation pattern of the proposed dual-polarized antenna fed through (a) Port 1 in  $xoz$ -plane, (b) Port 1 in  $xoy$ -plane, (c) Port 2 in  $xoz$ -plane, and (d) Port 2 in  $xoy$ -plane at 5.96 GHz.

### B. Radiation Performance

The radiation patterns were measured by exciting only one port and connecting the other port to a  $50 \Omega$  match load. Fig. 9 presents the simulated and measured gains of the dual-polarized antenna in Fig. 8. It is seen from Fig. 9 that the antenna gain is greater than 10 dBi over the operating band ( $|S_{11}| < -10$  dB). The measured (simulated) maximum gain of this antenna is 10.9 dBi (11.5 dBi). The measured total efficiencies of the two ports are also shown in Fig. 9; here, we find that the maximum value can be up to 93.6%. Fig. 10 presents the simulated and measured radiation patterns for this antenna at 5.96 GHz. Fig. 10(a) and (b) presents the radiation patterns for the horizontal polarization, and Fig. 10(c) and (d) depicts the ones for the vertical polarization. It is seen that measured radiation

TABLE II  
COMPARISONS BETWEEN THE PROPOSED DESIGN AND REPORTED WORKS

Ref	Type	Volume ( $\lambda_0^3$ )	BW (%)	Max Gain (dBi)	Gain/Area ( $1/\lambda_0^2$ )
[19]	Single	$1.66*1.66*0.031$	2.6%	10.6	4.17
[28]	Single	$2.20*2.88*0.011$	NG	10.0	1.58
[29]	Single	$2.83*2.83*0.085$	17.6%	11.84	1.91
[30]	Single	$\pi*(1.33)^2*0.037$	1.2%	10.19	1.88
<b>This work</b>	<b>Dual</b>	<b><math>1.65*1.65*0.040</math></b>	<b>3.0%</b>	<b>11.5</b>	<b>5.19</b>

NG: not given; Single: single-polarized; Dual: dual-polarized.

patterns agree well with simulated results. The antenna achieves a sidelobe level of  $-12$  dB and the cross-polarization level of less than  $-20$  dB in the broadside direction. In addition, the maximum value of envelop correlation coefficient calculated from the radiation patterns [32] is only 0.0498 over the entire operating band, which is much smaller than the requirement of MIMO systems.

### C. Comparisons

A comparative study of the proposed antenna with other high-gain antenna designs is presented in Table II, in terms of antenna structure, volume, bandwidth, maximum gain, and the ratio of Gain-to-Area (which describes the utilization ratio of the aperture). For making a fair comparison, the board area of the antennas includes also the area of the ground plane. The shorting-pin loading technique reported in [19] can only enhance the gain of the patch antenna operating in the fundamental mode, thus, limiting its possibility to excite high-order modes and achieve further gain enhancement. The chessboard structure reported in [28], although having a high gain (11.84 dBi), is not suitable for the dual-polarized operation. The high-gain antenna based on two stacked circular patches [30] is rather bulky and single polarized. Inspired by the gain-enhancement mechanism in [30], we propose here a high-gain, low-profile rectangular antenna, which requires only a single-dielectric layer and a simple feed, while achieving a higher ratio of Gain-to-Area. Most importantly, our design is suitable for a dual-polarized operation with satisfactory isolation.

## IV. CONCLUSION

In this letter, we propose a high-gain, low-profile dual-polarized microstrip antenna, which consists of dual orthogonal radiating elements (which excite the  $TM_{50}$  mode) loaded with slots (which effectively excite the  $TM_{10}$  mode). The proposed antenna can not only achieve the gain enhancement, but also possess unique features, such as single-layered, low-cost, and low-profile. The maximum gain of 10.9 dBi is measured at 5.96 GHz, even though the prototyped antenna has a size of only  $1.65 \lambda_0 \times 1.65 \lambda_0 \times 0.04 \lambda_0$ . Last but not least, the proposed dual-polarized antenna does not require complex feeding networks and stacked configurations, while offering high isolation, high broadside gain, and low sidelobes.

## REFERENCES

- [1] M. A. Jensen and J. W. Wallace, "A review of antennas and propagation for MIMO wireless communication," *IEEE Trans. Antennas Propag.*, vol. 52, no. 11, pp. 2810–2824, Nov. 2004.
- [2] J. F. Valenzuela-Valdés, M. A. García-Fernández, A. M. Martí González, and D. A. Sánchez-Hernández, "Evaluation of true polarization diversity for MIMO systems," *IEEE Trans. Antennas Propag.*, vol. 57, no. 9, pp. 2746–2755, Sep. 2009.
- [3] P. S. Kildal and K. Rosengran, "Correlation and capacity of MIMO systems and mutual coupling, radiation efficiency, and diversity gain of their antennas: Simulations and measurements in a reverberation chamber," *IEEE Commun. Mag.*, vol. 42, no. 12, pp. 102–112, Dec. 2004.
- [4] S. C. K. Ko and R. D. Murch, "Compact integration diversity antenna for wireless communications," *IEEE Trans. Antennas Propag.*, vol. 49, no. 6, pp. 954–960, Jun. 2001.
- [5] K.-M. Mak, H. Wong, and K.-M. Luk, "A shorted bowtie patch antenna with a cross dipole for dual polarization," *IEEE Antennas Wireless Propag. Lett.*, vol. 6, pp. 126–129, 2007.
- [6] Y. Liu, H. Yi, F. W. Wang, and S. X. Gong, "A novel miniaturized broadband dual-polarized dipole antenna for base station," *IEEE Antennas Wireless Propag. Lett.*, vol. 12, pp. 1335–1338, 2013.
- [7] Y. Gou, S. Yang, J. Li, and Z. Nie, "A compact dual-polarized printed dipole antenna with high isolation for wideband base station applications," *IEEE Trans. Antennas Propag.*, vol. 62, no. 8, pp. 4392–4395, Aug. 2014.
- [8] Y. Cui, X. Gao, H. Fu, Q.-X. Chu, and R. Li, "Broadband dual-polarized dual-dipole planar antennas: Analysis, design, and application for base stations," *IEEE Antennas Propag. Mag.*, vol. 59, no. 6, pp. 77–87, Dec. 2017.
- [9] Y. Li, Z. J. Zhang, J. F. Zheng, and Z. H. Feng, "Compact azimuthal omnidirectional dual-polarized antenna using highly isolated colocated slots," *IEEE Trans. Antennas Propag.*, vol. 60, no. 9, pp. 4037–4045, Sep. 2012.
- [10] Y. Li, Z. Zhang, W. Chen, Z. Feng, and M. F. Iskander, "A dual-polarization slot antenna using a compact CPW feeding structure," *IEEE Antennas Wireless Propag. Lett.*, vol. 9, pp. 191–194, 2010.
- [11] Y. Li, Z. Zhang, C. Deng, Z. Feng, and M. F. Iskander, "2-D planar scalable dual-polarized series-fed slot antenna array using single substrate," *IEEE Trans. Antennas Propag.*, vol. 62, no. 4, pp. 2280–2283, Apr. 2014.
- [12] Q. Xue, S. Liao, and J. Xu, "A differentially-driven dual-polarized magneto-electric dipole antenna," *IEEE Trans. Antennas Propag.*, vol. 61, no. 1, pp. 425–430, Jan. 2013.
- [13] S. G. Zhou, Z. H. Peng, G. L. Huang, and C. Y. Sim, "Design of a novel wideband and dual polarized magnetolectric dipole antenna," *IEEE Trans. Antennas Propag.*, vol. 65, no. 5, pp. 2645–2649, Mar. 2017.
- [14] Q. Wu and K. M. Luk, "A broadband dual-polarized magnetolectric dipole antenna with simple feeds," *IEEE Antennas Wireless Propag. Lett.*, vol. 8, pp. 60–63, 2009.
- [15] K. D. M. Pozar and D. H. Schaubert, *Microstrip Antennas: The Analysis and Design of Microstrip Antennas and Arrays*. New York, NY, USA: IEEE, 1995.
- [16] Z. Tang, J. Liu, Y.-M. Cai, J. Wang, and Y. Yin, "A wideband differentially fed dual-polarized stacked patch antenna with tuned slot excitations," *IEEE Trans. Antennas Propag.*, vol. 66, no. 4, pp. 2055–2060, Apr. 2018.
- [17] Q. Li, S. W. Cheung, and C. Zhou, "A low-profile dual-polarized patch antenna with stable radiation pattern using ground-slot groups and metallic ground wall," *IEEE Trans. Antennas Propag.*, vol. 65, no. 10, pp. 5061–5068, Oct. 2017.
- [18] D. Sun, Z. Zhang, X. Yan, and X. Jiang, "Design of broadband dual-polarized patch antenna with backed square annular cavity," *IEEE Trans. Antennas Propag.*, vol. 64, no. 1, pp. 43–52, Jan. 2016.
- [19] X. Zhang and L. Zhu, "Gain-enhanced patch antennas with loading of shorting pins," *IEEE Trans. Antennas Propag.*, vol. 64, no. 8, pp. 3310–3318, Aug. 2016.
- [20] H.-D. Chen, C.-Y.-D. Sim, and J.-Y. Wu, "Broadband high-gain microstrip array antennas for WiMAX base station," *IEEE Trans. Antennas Propag.*, vol. 60, no. 8, pp. 3977–3980, Aug. 2012.
- [21] J. Huang, "A Ka-band circularly polarized high-gain microstrip array antenna," *IEEE Trans. Antennas Propag.*, vol. 43, no. 1, pp. 113–116, Jan. 1995.
- [22] X. P. Chen, K. Wu, L. Han, and F. F. He, "Low-cost high gain planar antenna array for 60-GHz band applications," *IEEE Trans. Antennas Propag.*, vol. 58, no. 6, pp. 2126–2129, Jun. 2010.
- [23] L. Chang, Z. Zhang, Y. Li, and Z. Feng, "Air substrate 2-D planar cavity antenna with chessboard structure," *IEEE Antennas Wireless Propag. Lett.*, vol. 16, pp. 321–324, 2017.
- [24] L. Chang, Z. Zhang, Y. Li, and M. F. Iskander, "Air substrate slot array based on channelized coplanar waveguide," *IEEE Antennas Wireless Propag. Lett.*, vol. 16, pp. 892–895, 2017.
- [25] L. Herve and L. Shafai, "New stacked microstrip antenna with large bandwidth and high gain," *IEE Proc. Microw. Antennas Propag.*, vol. 141, no. 3, pp. 199–204, 1994.
- [26] V. P. Sarin, M. S. Nishamol, D. Tony, C. K. Aanandan, P. Mohanan, and K. Vasudevan, "A wideband stacked offset microstrip antenna with improved gain and low cross polarization," *IEEE Trans. Antennas Propag.*, vol. 59, no. 4, pp. 1376–1379, Jan. 2011.
- [27] E. Nishiyama and M. Aikawa, "Wide-band and high-gain microstrip antenna with thick parasitic patch substrate," in *Proc. Int. Symp. IEEE Antennas Propag. Soc.*, Jun. 2004, pp. 273–276.
- [28] R. Q. Lee, R. Acosta, and K. F. Lee, "Radiation characteristics of microstrip arrays with parasitic elements," *Electron. Lett.*, vol. 23, pp. 835–837, 1987.
- [29] Q. U. Khan, M. B. Ihsan, D. Fazal, F. M. Malik, S. A. Sheikh, and M. Salman, "Higher order modes: A solution for high gain, wide band patch antennas for different vehicular applications," *IEEE Trans. Veh. Technol.*, vol. 66, no. 5, pp. 3548–3554, May 2017.
- [30] P. Juyal and L. Shafai, "A high gain single feed dual mode microstrip disc radiator," *IEEE Trans. Antennas Propag.*, vol. 64, no. 6, pp. 2115–2126, Jun. 2016.
- [31] X. Zhang, L. Zhu, and Q.-S. Wu, "Side-lobe-reduced and gain-enhanced square patch antennas with adjustable beamwidth under  $TM_{03}$  mode operation," *IEEE Trans. Antennas Propag.*, vol. 66, no. 4, pp. 1704–1713, Apr. 2018.
- [32] Y. Gao, X. Chen, Z. Ying, and C. Parini, "Design and performance investigation of a dual-element PIFA array at 2.5 GHz for MIMO terminal," *IEEE Trans. Antennas Propag.*, vol. 55, no. 12, pp. 3433–3441, Dec. 2007.